Smart Materials and Structures

Electrically controllable connection and power transfer by electroadhesion

OPEN ACCESS
IOP Publishing
Smart Materials and Structures
Smart Mater. Struct. **28** (2019) 105012 (7pp)
https://doi.org/10.1088/1361-665X/ab383b

Electrically controllable connection and power transfer by electroadhesion

Jianglong Guo[1], **Chaoqun Xiang**[1] **and Jonathan Rossiter**

SoftLab, Bristol Robotics Laboratory, University of Bristol, Bristol, United Kingdom

E-mail: J.Guo@bristol.ac.uk

Received 5 May 2019, revised 23 July 2019
Accepted for publication 2 August 2019
Published 29 August 2019

Abstract

Reconfigurable smart structures and robots require interconnects that enable the transfer of forces, power and data from one modular element to another. This is typically achieved through magnetic coupling, mechanical clips and male–female electrical contacts. In lightweight structures however, these methods are impractical due to weight and complexity. In this work we present an electroadhesive coupling (EAC) controllable interfacial connection for joining lightweight modular components, which enable simultaneous mechanical joining and electrical pass-through connections for power and communication. Active adhesion and power transfer are realized by electroadhesion (EA) using conducting electrodes on lightweight materials such as papers. We present the underlying EAC concept, materials and structures, and demonstrate this new approach using origami and kirigami structures to fabricate a modular EAC bridge and a modular EAC cuboid structural interconnection system. These novel structures have the potential for application in lightweight robotics, space systems, deployable and self-assembling and self-disassembling systems.

Supplementary material for this article is available online

Keywords: active connection, active power transfer, electroadhesion, electroadhesive interconnect

(Some figures may appear in colour only in the online journal)

1. Introduction

Modular robots usually consist of repeated robotic modules connected together to provide versatile and configurable robotic systems that can form different structures with different capabilities, and which can adapt to unknown and unstructured environments [1]. There are four critical elements associated with a typical modular robotic system: (1) a docking element that allows physical connections between modules, (2) a locomotion element that permits the docking function, (3) a computation element that offers control of the locomotion and docking and communication between modules, and (4) a power element for the computation system [2].

Traditional interconnects that enable the transfer of forces, power, and data from one robotic module to another include magnetic coupling, mechanical clips, and male–female electrical contacts [2–5]. This limits the weight and design of the robots. There is, therefore, a need for lighter, simpler and lower cost modular interconnection technologies. Electroadhesion (EA) [6] is an attractive and electrically controllable adhesion technology that has been widely employed in material handling [7–11], climbing robotics [12–14], and active attachment [15–20] applications due to the fact that: (1) EA pads can be produced using lightweight materials and simple structures, (2) the energy consumption of EA is low (in the range of mW), and (3) EA can be used on a wide range of surfaces and to lift almost any materials, including conductive and insulating materials. Electroadhesion is a controllable technology with potential for use in interconnecting lightweight modular robotics systems.

[1] These authors contributed equally to the work.

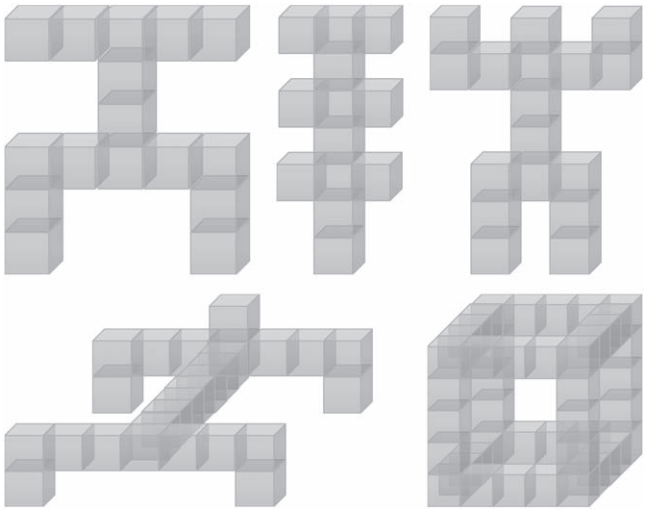

Figure 1. Example lightweight modular structure designs.

An EA pad is typically fabricated as a pair of spaced coplanar electrodes embedded in a dielectric. When an EA pad is in contact with or close to (in the range of mm) a substrate material and a high voltage (in the range of kV) is applied between the electrodes, counter charges are induced at the surface of the substrate, causing EA attractive forces between the EA pad and the substrate [8, 21]. De-adhesion or release between two surfaces can be achieved by switching off the high voltage power supply. This on–off characteristic can be exploited as an electrically controllable and active connection mechanism for joining parts [17, 20], such as lightweight modular structures and systems shown in figure 1.

Germann *et al* utilized EA for connecting two plastic balloons to show the potential of using EA as an active connection method for soft modular robotic applications [17]. Multiple high voltage channels are, however, required to connect several soft modules together as the EA electrodes are arranged in the inner side of the balloons. Karagozler *et al* proposed the use of electrostatic latching for physical connection, power transfer, and communication between modules. The adhesion between modules was based on electrostatic forces between parallel capacitors. Power transfer and communication were based on capacitive coupling, which required complex associated electronic circuits [20]. Here we demonstrate novel lightweight designs and soft-smart structures using only one high voltage channel to induce coplanar EA for controllable modular connection and power transfer. We term this simultaneous electrical and mechanical coupling ***electroadhesive coupling*** (EAC).

EAC structures are lightweight and easy to fabricate using folded laminar materials and ultra-lightweight foam blocks such as aerogels [22]. A simple embodiment of the EAC system is as an origami cube made from paper (or similar sheet insulator) and conducting electrical tracks, such as conductive inks [23] or adhesive metal foils. The EAC concept is shown in figure 2. This concept can be used to connect the modular elements shown in figure 1 to form systems with different structures. An EAC connection is enabled from the face which is initially connected to a high voltage amplifier (HVA) (termed the driving face) and which, upon completion of the connection, is

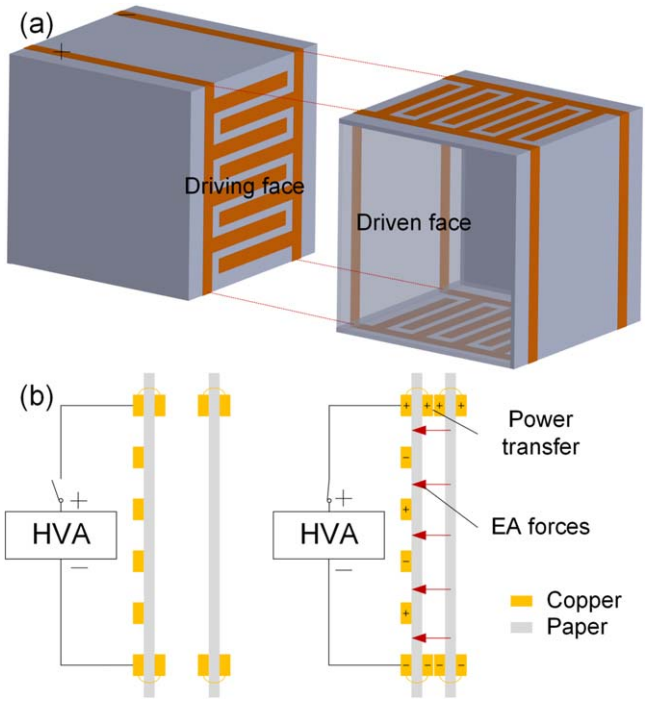

Figure 2. EAC concept. (a) Two cubic EAC modules in 3D. (b) Cross-sectional view of the EAC interface when HV us off (left) and on (right).

connected to the second face (termed the driven face) due to the employment of electroadhesion (see figure 2(b)).

The EAC interfacial interconnect employs two components: (1) two peripheral electrodes, presented on both driving and driven faces, that permit the pass-through of electrical supply from one face to the next (and hence from one module to the next) and (2) a central interdigitated region present on the driving face which induces electroadhesive forces between it and the driven face. The key benefits of this structure include (1) only one HVA channel is needed for both active connection and power transfer between lightweight modules, (2) no heavy mechanical connections or magnets are needed, and (3) the potential for communication to be transmitted through the power lines from one module to the next using established power line communication (PLC) protocols [24]. This approach can be used to greatly reduce the weight, complexity and cost of the whole modular connection system.

The reminder of this article is organized as follows. EAC facial interconnection design, fabrication details and electroadhesive force test are presented in section 2. Case studies of the EAC interconnection and active power transfer concept are described in section 3. Discussions on how to increase number of connected modules and further application of laminar (e.g. paper) electroadhesion for multi-part connected structures are demonstrated in section 4. Conclusions and future work are outlined in section 5.

2. EA pad design, fabrication, and force test

EAC components can be readily fabricated using low cost commercially available metal tapes and laminar materials.

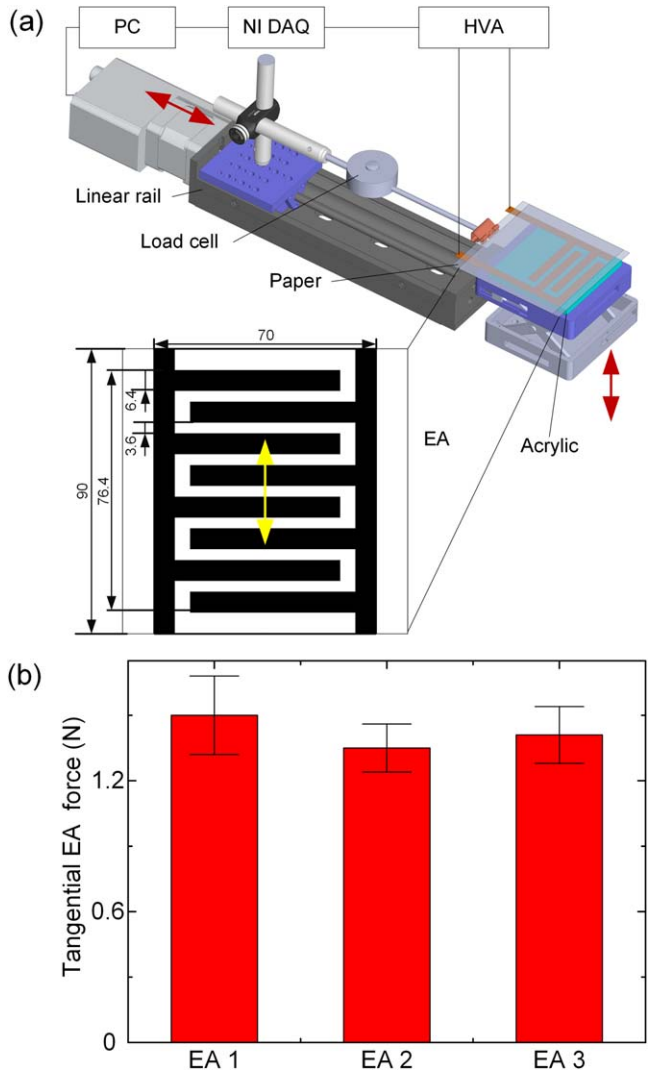

Figure 3. Tangential EA force measurement rig and fabrication repeatability. (a) Schematic diagram of the tangential force measurement device. Inset shows EA pad design and dimensions tests. Yellow arrow shows the direction of movement. (b) Measured tangential forces of three EA pads with the same geometry and dimensions shown in (a). Mean and one std deviation for five tests are shown.

Here we demonstrate fabrication using copper tape and office paper. Firstly, we printed an EA electrode geometry onto A4 paper based on pre-defined electrode dimensions that were designed in SolidWorks. Strips of 6.4 mm wide off-the-shelf copper tape were used as electrodes. The space between electrodes was 3.6 mm (see figure 3(a)), since larger EA forces can be achieved when the electrode width/space ratio is around 1.8 [21]. Secondly, we manually cut the paper into designated sizes and bonded the copper tapes onto them based on the printed electrode patterns.

In order to test the repeatability of the proposed EA fabrication method, we establised a tangential EA force measurement apparatus, as shown in figure 3(a). We utilised an inline miniature S-Beam load cell (Applied Measurements Ltd, UK) to measure the adhesive force. We applied a linear rail (X-LSQ150B-E01, Zaber Technologies Inc., USA) to pull a piece of office paper away from the EA pad after charging for 30 s at 3.2 kV using an Ultravolt 5HVA24-BP high voltage power supply (Advanced Energy Industries, Inc., USA). The movement speed was 50 mm s^{-1}. We used a NI USB-6343 X Series DAQ device (National Instruments, UK) to record the adhesive forces and control the output voltage of the HVA.

We then fabricated three EA pads using the same procedure and same geometry and dimensions. The overall effective electrode area of the EA pads was 76.4 mm × 70 mm, as shown in figure 3(a). Five tests were conducted for each EA pad. All tests were conducted at an enclosed customized high voltage box. During the EA force measurement, the temperature was 21.7 °C ± 0.1 °C and relative humidity was 53% ± 1% using a weather station. We measured the tangential EA force when high voltage was applied to the EA pads. The results can be seen in figure 3(b), where there was a maximum relative difference of 11.1% in the average tangential EA forces obtained across the three EA pads. This difference can be further minimized by using advanced EA pad fabrication methods, such as flexible printed circuit board manufacturing approaches [21, 25].

3. EAC active power transfer and connection case studies

3.1. EAC bridge

The simplest modular EAC structure employs flat sheets made of an unfolded paper with two simple interdigitated copper tape electrodes, as shown in figure 4(a). When a voltage is applied to the electrodes, the paper and copper tape composite forms an EA adhesive patch that can be used to attach to the next planar module. When the second module is attached, the copper tapes on the two modules connect and power is then supplied to the EA patch on the second module, ready for it to attach to the next, and so on until a chain of modules of the required length is formed. The first and/or last EA patch can be optionally connected to a fixed substrate, providing anchoring points for the structure.

Based on this chaining principle, we fabricated an EA bridge, as shown in figure 4(b), where we joined 6 EA modules to cross a gap between two stands. Each module weighed only 1.5 g and we used an EMCO E60 HVA (EMCO High Voltage Corporation, USA, maximum voltage of 6 kV) to deliver the high voltage (3.2 kV in this case) to the electrodes. The bridge was strong enough to support itself and a rubber duck of mass 5.5 g. The EA bridge remained connected while the high voltage as applied. When we removed the voltage, adhesion between all units decayed to nothing and the bridge collapsed, as shown in figure 4(c). Please see the demonstration of this in the supplementary video is available online at stacks.iop.org/SMS/28/105012/mmedia.

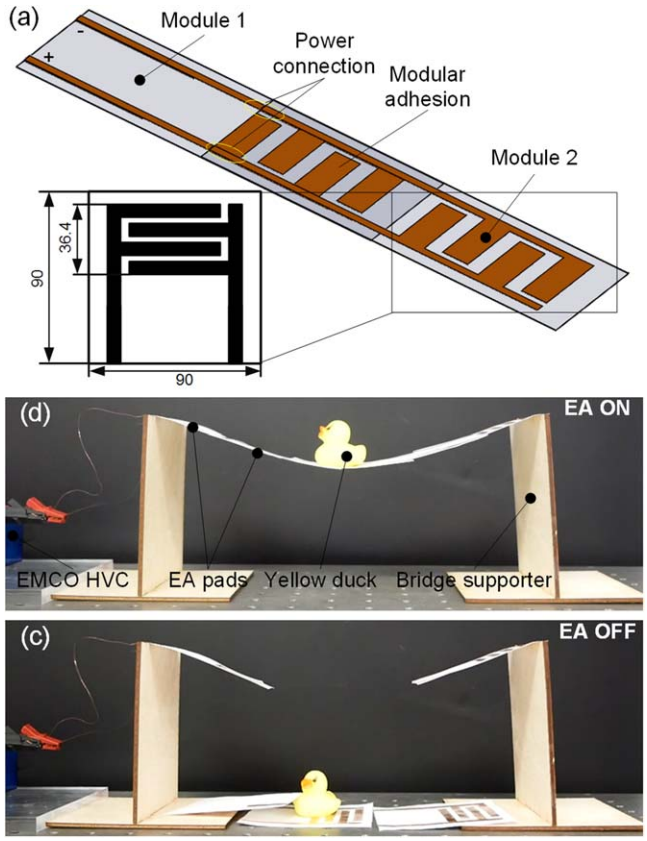

Figure 4. The EAC bridge design and prototype. (a) 3D diagram of an EAC planar module chain with two modules. Inset shows the EAC module design. (b) Prototype of the EA bridge when 3.2 kV was applied. (c) The collapsed EA bridge when the voltage was turned off.

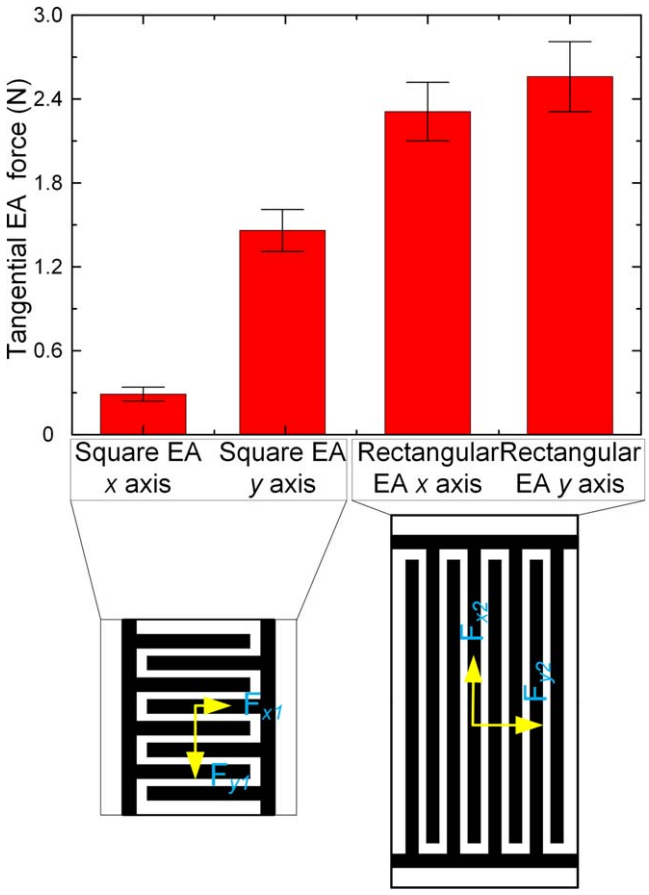

Figure 5. Tangential EA forces in x and y axis directions for the near square interdigital EA design and the improved rectangular interdigital EA design.

3.2. Cuboid EAC modules

Previous results have shown that the tangential EA force along the direction of the electrode lines (here labelled the y axis) is greater than the force normal to electrode lines (here labelled the x axis) for interdigital EA electrode designs [17]. We measured the tangential EA force of an EA pad (the same design used in figure 3(a)) in both the x axis and y axis direction and found that, for the near squared EA pad design described in figure 3(a), the relative difference in the amount of adhesive force in the x axis and y axis was 403.4%, as presented in figure 5. We define the relative difference as: (tangential EA force in the y axis - tangential EA force in the x axis)/tangential EA force in the x axis $\times$ 100%. We assume we could achieve similar amount of tangential EA force in both axes by increasing the electrode length in the x direction. We therefore extended the electrode length from 70 to 160 mm and found that for the improved design, only a relative difference of 10.8% was obtained. Comparison between these two EA shapes is shown in figure 5.

Based on the improved rectangular interdigital EA design, we designed and fabricated several cuboid EAC modules. We define two module types: Type A, with EA pads on two opposing faces; and Type B, with no EA pads but with electrical interconnects (see figure 6(a)). The total mass of the Type A cuboid module was 7.4 g (mass of electrodes: 3.0 g)

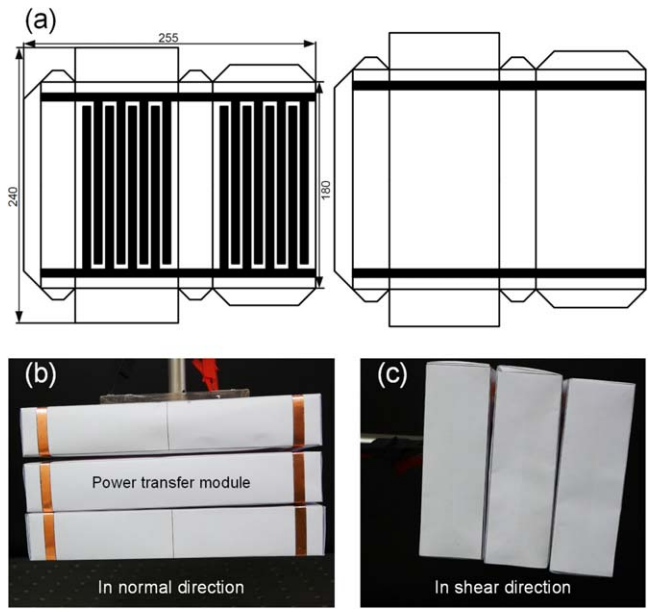

Figure 6. Cuboid EA modular robot designs and prototypes. (a) Design of the Type A EAC cuboid module with two EA faces, and Type B with only power transfer electrodes. (b) Three connected cuboid EAC modules in normal direction. (c) Three connected cuboid EAC modules in shear direction.

and the mass of the Type B module was 5.0 g (mass of electrodes: 0.6 g).

To demonstrate how modules can be connected, we fixed one Type A EAC module and applied a high voltage (3.2 kV) to its electrodes. We then touched a second module of Type B to the underside of the fixed module, to which it adhered due to the EA force generated by the Type A (please see the supplementary video). We then touched a second Type A module to the previously attached Types B module, to which it attached by generating its own EA force. We define the normal direction in line with gravity, and the shear direction as the direction perpendicular to gravity. Three origami cuboid modules can be attached in both normal, as shown in figure 6(b), and shear directions, as shown in figure 6(c). In order to investigate the maximum mass one EAC module can carry, given the EAC Type A design shown in figure 6(a), we increased the applied voltages to 4 kV (higher voltages may induce electric discharges) and found that the maximum mass the EA side of one EAC Type A module can carry was 16.8 g at 4 kV.

4. Discussion

Taking the normal direction as an example, we assume the maximum normal force an EA module can generate is F_{EANmax} for an EAC module with a volume of V and density ρ. We assume that the contact between touching EAC modules is perfectly flat (although in real cases, peeling and paper bending should be considered, as shown in figure 7(a)). We therefore have a limit on the number of EAC modules that can be held, defined by the inequality:

$$F_{\mathrm{EAN\,max}} > n\rho Vg, \tag{1}$$

where n is the number of EAC modules that can be held and g is gravitational acceleration (9.81 ms^{-2} used in this paper).

F_{EANmax} is usually proportional to the effective EA area of the modules. Expanding the effective EA electrode area will, therefore, enable the attachment of more modules. For the EAC Type A modules, with a fixed EA pattern, and thus a fixed F_{EANmax} and V, the number of EAC modules that can be held is:

$$n = \mathrm{floor}\left(\frac{F_{\mathrm{EAN\,max}}}{\rho Vg}\right) = \mathrm{floor}\left(\frac{34.6}{\rho}\right), \tag{2}$$

where, in this study, $V = 0.000\,486$ m^3 and $F_{\mathrm{EANmax}} = 0.165$ N.

Based on the equation (2), given a fixed maximum normal EA adhesive force of 0.165 N and a fixed module volume of 0.000 486 m^3, the relationship between the number of EAC modules and the density of module is plotted in figure 7(b). For the used EAC Type A modules, $\rho = 12.76$ kg m^{-3}, then the maximum number of serially-connected Type A EAC modules is: $n = 2$. The employment of lower density EAC modules, with lighter electrodes (such as carbon black) and dielectric materials (such as aerogel sheets, with density as low as 1 kg m^{-1}), will increase the number of units that can be jointed, as shown in figure 7(b). We measured the capacitance of the EAC Type A module through an LCR meter (E4980AL, Keysight Technologies, USA) under 1 V and 20 Hz. The energy stored can be calculated from:

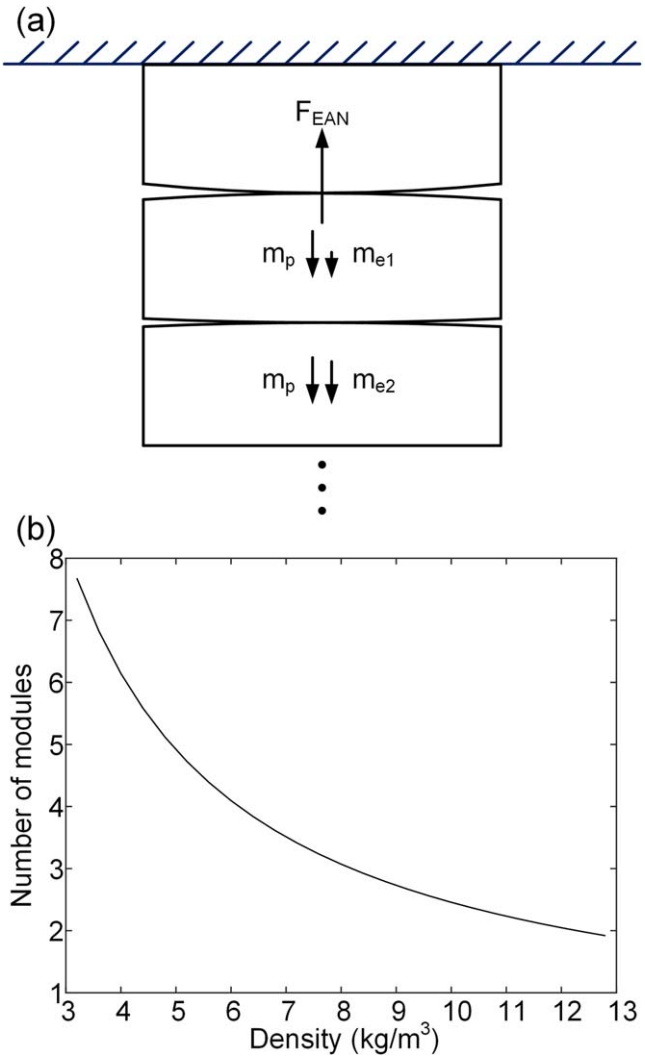

Figure 7. Force analysis of cuboid EA modular robots. (a) Schematic diagram of the force analysis of the EA modular robots in real cases, where F_{EAN} is the normal EA force, m_p is the mass of the paper part of the EA module, m_{e1} and m_{e2} are the masses of the electrode part of the Type B and A module respectively. (b) The relationship between the number of EAC Type A modules that can be serially connected and the module density based on equation (2) (under a fixed maximum normal EA adhesive force of 0.165 N and fixed module volume of 0.000 486 m^3).

$$W = 0.5CU^2, \tag{3}$$

where C is the capacitance value and U the voltage applied.

From equation (3), given the measured capacitance of 35.5 pF for the EAC Type A module and a voltage of 4 kV, the energy stored is 284 μJ. In addition, the current running through the electrodes is in the microamps range. The stored energy and current both represent very low risk to human beings and are well within the health and safety requirements [25]. However, due to the voltages used, individuals with

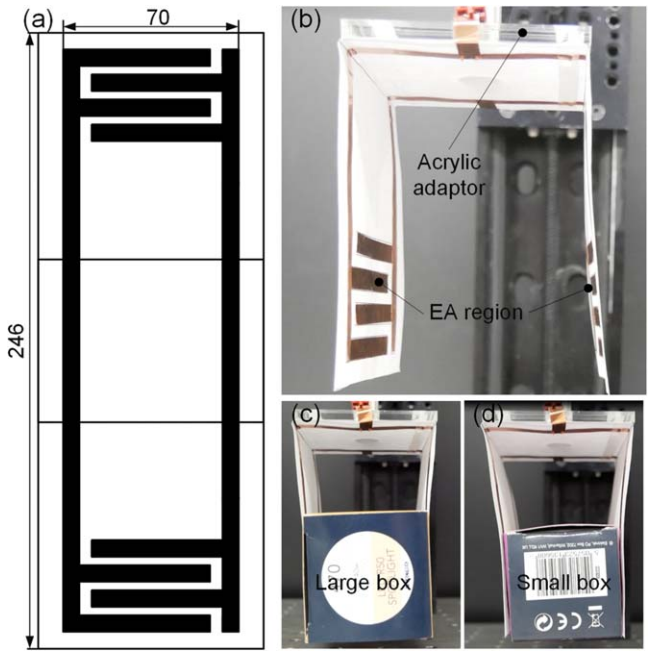

Figure 8. Origami EA gripper design and grasping performance evaluation. (a) Design and dimensions of the origami EA gripper. (b) Prototype of the origami EA gripper. (c) Grasping a large 35.6 g light bulb box at 3.6 kV. (d) Grasping a small 42.9 g light bulb box at 4 kV.

pacemakers are recommended to avoid handling these EAC modules. For space applications the number of connected modules is unlimited since no gravitational force acts in the static state and large complex modular structures can be constructed. More careful designs should be considered when space applications involve movement, where inertia effects must also be taken into account.

Paper has been adopted to fabricate cost-effective and lightweight actuators [26], robots [27, 28], and adhesion devices [29]. Paper electroadhesion can also be used to develop a simple and low-cost flexible EA gripper for adaptive grasping applications. In order to demonstrate how a gripper can be integrated into our proposed EAC modular system we designed a paper-based origami EAC gripper. The design and dimensions of the gripper and its prototype are shown in figures 8(a) and (b) respectively. The gripper weighed only 3.3 g. Since paper is flexible, it can be passively conformed to curved surfaces. Where shape adaptation under EA activation is not sufficient, actuators such as shape memory alloys can be used for shape conforming in order to grasp objects with a larger range of shapes. In this study the gripper can be used to grasp not only a large box (55 mm × 55 mm × 100 mm, 35.6 g) but also a smaller but heavier box (48 mm × 48 mm × 86 mm, 42.9 g). At its base the origami EA gripper was bonded to a 5 mm thick acrylic adaptor plate and connected to a vertical linear rail. When grasping the large box, as shown in figure 8(c), 3.6 kV was applied. When grasping the smaller, heavier box, as shown in figure 8(d), 4 kV was applied. Please see the grasping demonstrations in the supplementary video.

5. Conclusions and future work

Modular robotics have the potential to change how robots are made, how they grow and adapt, and how they can be decomposed and reused. Conventional modular robots predominantly use electromagnets [4] and mechanical connections [5] to join multiple modules. This limits the weight and design of the robots. In contrast here we have proposed an active, electrically controllable, lightweight, and cost-effective connection and concurrent power transfer mechanism for lightweight modular robots and structures. We have demonstrated the EAC system in origami and kirigami structures using low cost metal tapes and office papers. We have shown the underlying active and electrically controllable connection mechanism in an EAC modular bridge, modular cuboid elements series-connected by EA only, and a low-cost, shape-adaptive, paper-based origami EA gripper. The proposed fabrication methods are simple and relatively repeatable, showing a maximum difference of 11.1% observed in tangential EA forces tests. We have increased EA force generation by extending the electrode length, reducing force anisotropy from 403.4% for a square interdigital EA design to 10.8% for the improved rectangular design. Finally, we have observed that our paper-based origami EA gripper has passive shape adaptive capability. The 3.3 g origami EA gripper was able to lift a 42.9 g mass using 4 kV. These soft-smart structures have the potential to enable a wide variety of low-cost solutions to deployable structures and adaptive modular robotics.

The contributions of this paper include: (1) the concept and presentation of a novel electrically controllable, lightweight, and cost-effective connection and concurrent power transfer mechanism realized by low-cost and easy-to-fabricate paper electroadhesion; (2) the development of an EAC bridge; (3) the development of a modular cuboid assembly system exploiting an improved interdigital EA electrode pattern; and (4) the development of a paper-based origami EA gripper for shape-adaptive grasping. Future work will include studies into active self-folding EAC origami modular robots via shape memory alloys, exploiting lighter materials such as conductive inks and aerogels in order to increase the number of connected EAC modules, and equipping EAC modules with mobility in order to realise more complex and autonomous self-assembly. A static EA pad in air is essentially a capacitor in parallel with a resistor, which is similar to dielectric elastomer actuators [30]. We will implement the automatic identification of EAC module attachment by embedding the EAC module with capacitive self-sensing methods [31, 32]. Furthermore, data communication between EAC modules will be pursued using established PLC protocols.

Acknowledgments

The authors acknowledge support from EP/M020460/1 and EP/R02961X/1. Jonathan Rossiter is also supported by the Royal Academy of Engineering as a Chair in Emerging

Technologies. In addition, the authors thank the useful comments from the referees. All underlying data are provided in the main text within this paper and as supplementary information accompanying this paper.

ORCID iDs

Jianglong Guo https://orcid.org/0000-0002-9997-6059

References

[1] Daudelin J, Jing G Y, Tosun T, Yim M, Kress-Gazit H and Campbel M 2018 An integrated system for perception-driven autonomy with modular robots *Sci. Robot* **3** eaat4983
[2] Brunete A, Ranganath A, Segovia S, Frutos J P, Hernando M and Gambao E 2017 Current trends in reconfigurable modular robots design *J. Intell. Robotic Syst.* **14** 1–21
[3] Chennareddy S S R, Agrawal A and Karuppiah A 2017 Modular self-reconfigurable robotic systems: a survey on hardware architectures *J Robot* **2017** 5013532
[4] Gilpin K, Knaian A and Rus D 2010 Robot pebbles: one centimeter modules for programmable matter through self-disassembly 2010 *IEEE Int. Conf. on Robotics & Automation (ICRA 2010)* pp 2485–92
[5] Parrott C, Dodd T J and Groß R 2014 HiGen: a high-speed genderless mechanical connection mechanism with single-sided disconnect for self-reconfigurable modular robots 2014 *IEEE/RSJ Int. Conf. on Intelligent Robots and Systems (IROS 2014)* pp 3926–32
[6] Rahbek K 1935 Electroadhesion apparatus *US Patent* 2025123A
[7] Monkman G J, Hesse S, Steinmann R and Schunk H 2007 *Robot Grippers* (New York : Wiley)
[8] Monkman G 1997 An analysis of astrictive prehension *Int. J. Robot. Res.* **16** 1–10
[9] Guo J L, Bamber T, Zhao Y C, Chamberlain M, Justham L and Jackson M 2017 Toward adaptive and intelligent electroadhesives for robotic material handling *IEEE Robot. Autom. Lett.* **2** 538–45
[10] Guo J L, Elgeneidy K, Xiang C Q, Lohse L, Justham L and Rossiter J 2018 Soft pneumatic grippers embedded with stretchable electroadhesion *Smart Mater. Struct.* **27** 055006
[11] Guo J L, Xiang C Q and Rossiter J 2018 A soft and shape-adaptive electroadhesive composite gripper with proprioceptive and exteroceptive capabilities *Mater. Des.* **156** 586–7
[12] Wang H Q, Yamamoto A and Higuchi T 2014 A crawler climbing robot integrating electroadhesion and electrostatic actuation *Int. J. Adv. Robot. Syst.* **11** 191
[13] Liu R, Chen R, Shen H and Zhang R 2012 Wall climbing robot using electrostatic adhesion force generated by flexible interdigital electrodes *Int. J. Adv. Robot. Syst.* **10** 36
[14] Gu G Y, Zou J, Zhao R K, Zhao X H and Zhu X Y 2018 Soft wall-climbing robots *Sci. Robot.* **3** eaat2874
[15] Graule M A, Chirarattananon P, Fuller S B, Jafferis N T, Ma K Y, Spenko M, Kornbluh R and Wood R J 2016 Perching and takeoff of a robotic insect on overhangs using switchable electrostatic adhesion *Science* **352** 978–82
[16] Ruffatto D III, Glick P E, Tolley M T and Parness A 2018 Long-duration surface anchoring with a hybrid electrostatic and gecko-inspired adhesive *IEEE Robot. Autom. Lett.* **3** 4201–8
[17] Germann J, Dommer M, Pericet-Camara R and Floreano D 2012 Active connection mechanism for soft modular robots *Adv. Robot.* **26** 785–98
[18] Heath C J C, Bond I P and Potter K D 2016 Electrostatic adhesion for added functionality of composite structures *Smart Mater. Struct.* **25** 025016
[19] Leung B C, Goeser N R, Miller L A and Gonzalez S 2015 Validation of electroadhesion as a docking method for spacecraft and satellite servicing *2015 IEEE Aerosp Conf.* pp 1–8
[20] Karagozler M E, Campbell J D, Fedder G K, Goldstein S C, Weller M P and Yoon B W 2007 Electrostatic latching for inter-module adhesion, power transfer, and communication in modular robots *2007 IEEE/RSJ Int. Conf. on Intelligent Robots and Systems (IROS 2007)* pp 2779–86
[21] Guo J L, Bamber T, Chamberlain M, Justham L and Jackson M 2016 Optimization and experimental verification of coplanar interdigital electroadhesives *J. Phys. D: Appl. Phys.* **49** 415304
[22] Zhang H Y, Lyu S G, Zhou X M, Gu H B, Ma C, Wang C H and Ding T 2019 Super light 3D hierarchical nanocellulose aerogel foam with superior oil adsorption *J. Colloid Sci.* **536** 245–51
[23] Lessing J, Glavan A C, Walker S B, Keplinger C, Lewis J A and Whitesides G M 2014 Inkjet printing of conductive inks with high lateral resolution on omniphobic 'RF paper' for paper-based electronics and MEMS *Adv. Mater.* **26** 4677–82
[24] Faure J P, Allen J D, Stelts M, Rajkotia P, von Doenhoff R C, Horvath S and Gavette S 2010 *IEEE standard for broadband over power line networks: medium access control and physical layer specifications* IEEE Std 1901™-2010 (https://doi.org/10.1109/IEEESTD.2010.5678772)
[25] Pourazadi S, Shagerdmootaab A, Chan H, Moallem M and Menon C 2017 On the electrical safety of dielectric elastomer actuators in proximity to the human body *Smart Mater. Struct.* **26** 115007
[26] Ruffatto D, Shah J and Spenko M 2014 Increasing the adhesion force of electrostatic adhesives using optimized electrode geometry and a novel manufacturing process *J. Electrostat.* **72** 147–55
[27] Chen A S, Zhu H, Li Y, Hu L and Bergbreiter S 2014 A paper-based electrostatic zipper actuator for printable robots *2014 IEEE Int. Conf. on Robotics & Automation (ICRA)* pp 5038–43
[28] Shigemune H, Maeda S, Cacucciolo V, Iwata Y, Iwase E, Hashimoto S and Sugano S 2017 Printed paper robot driven by electrostatic actuator *IEEE Robot. Autom. Lett.* **2** 1001–7
[29] Wu Q, Pradeep V and Liu X 2018 A paper-based wall-climbing robot enabled by electrostatic adhesion 2018 *IEEE/RSJ Int. Conf. on Soft Robotics (RoboSoft 2018)* pp 315–20
[30] Kumar S and Santhanam V 2017 Inkjet printed electroadhesive pads on paper *Int. J. Nanotechnol.* **14** 859–65
[31] Gisby T A, O'Brien B M and Anderson I A 2013 Self sensing feedback for dielectric elastomer actuators *Appl. Phys. Lett.* **102** 193703
[32] Rizzello G, Naso D, York A and Seelecke S 2016 Closed loop control of dielectric elastomer actuators based on self-sensing displacement feedback *Smart Mater. Struct.* **25** 035034
[33] Cao C, Sun X, Fang Y, Qin Q, Yu A and Feng X 2016 Theoretical model and design of electroadhesive pad with interdigitated electrodes *Mater. Des.* **89** 485–91